

Modelling gravity waves in an aluminium reduction cell using OpenFoam

M. Dupuis, Jonquière, and Michaël Pagé, St-Nazaire

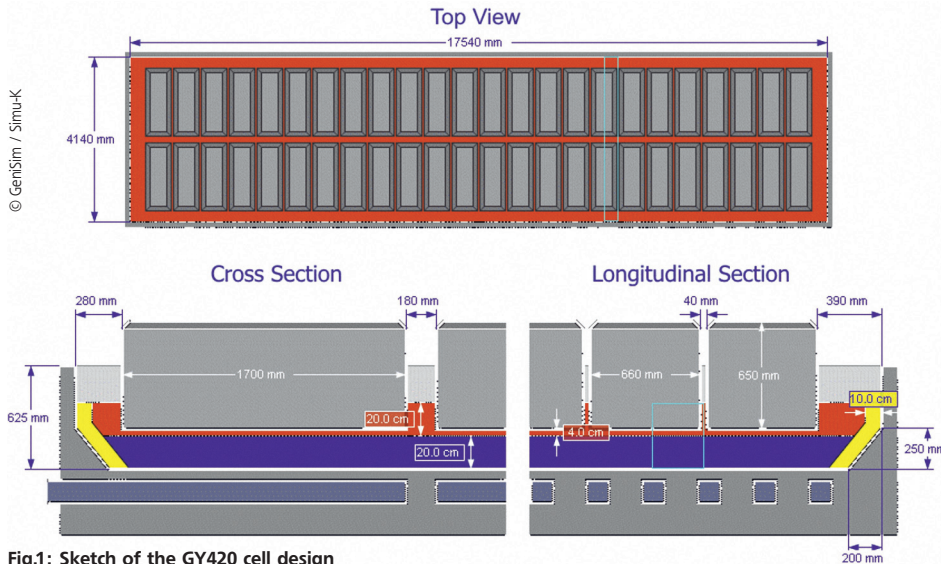


Fig.1: Sketch of the GY420 cell design

In recent years extensive computer modelling work has tried to establish whether using a profiled cathode surface modifies the MHD stability of an aluminium reduction cell. Two types of studies have been carried out: full 3D steady-state analysis, and shallow layer 2D transient analysis. Neither type of analysis is well suited to examine the effect of a profiled cathode surface on the cell stability. The present work proposes a new method to model relative MHD stability. Lateral gravity waves were simulated in a 3D lateral slice of an aluminium reduction cell. The model was solved by using the VOF formulation of the OpenFoam code. Results of the evolution of the bath-metal interface are presented for a reduction cell having different types of irregularity on the cathode surfaces. That interface evolution is compared to the flat cathode surface case; irregular surfaces provided little extra damping of the gravity waves.

The irregular cathode surface technology is under continual development in China [1]. A recent Chinese paper outlined a detailed 3D model based on ANSYS and CFX solvers [2]. Steady-state solutions were presented for a reduction cell with either a flat or an irregular cathode surface. Both MHD and gas release under the anodes were driving the fluid motion. The steady-state results of the 3D model with irregular cathode surface clearly dem-

onstrated that the bath and metal flows were three-dimensional in nature (see Fig. 12b of [2]).

Studies using a 2D transient model (MHD-Valdis, with bath and metal flows in two horizontal shallow layers) could not identify any significant impact of an irregular cathode surface on the cell stability [3-6]. This suggests either that using irregular cathode surface does not affect cell stability, or that cell instability depends on the three-dimensional flows introduced by irregular cathode surface and not taken into account by MHD-Valdis. Despite that limitation, MHD-Valdis remains an efficient stability analysis tool for standard cells with a flat cathode surface, and where the flows are essentially two-dimensional.

Since the bath-metal interface motion is a time-dependant phenomenon, a cell stability analysis should be based on a transient model. The above remarks indicate that in the case of an irregular cathode surface, the model should also be in 3D, since this type of cathode surface generates three-dimensional flows.

A new modelling approach

The variable Lorentz forces in the metal pad of a reduction cell drive the fluid movements, while viscous damping reduces the fluid movements [7, 8]. The aim of an irregular cathode surface would be to increase the viscous damping in the metal and thereby to enhance cell stability.

For a bath-metal interface wave to move around the cell, both molten metal and the bath volumes must move. Since the bath layer thickness under the anodes is much less deep than the metal pad thickness, the average speed of the bath flow there has to be greater than the average speed of the metal pad flow. Hence viscous damping in the bath is very important to the bath-metal interface wave dynamic, and must also be considered.

In view of the limitations of the models presently used for stability analysis of reduction cells with irregular cathodes surfaces, a new modelling approach was developed and tested. The new approach used a transient 3D model consisting of a lateral slice through a reduction cell. The bath and molten metal were subjected to lateral gravity waves by initially inclining the bath-metal interface. The cathode surface was either flat or with different versions of irregularities. The speeds of the bath and metal layers and the movement of the bath-metal interface were calculated over time.

Selection of a proper numerical code to simulate a free interface wave

Only a few codes are able to cope with the physics of the proposed model, which is a transient 3D multi-phase flow problem; the open source code OpenFoam is one of them. OpenFoam has become a popular code in many applications due to its free surface modelling capabilities [9], which are comparable to other VOF solvers like CFX [10].

The motion of the free interface between two immiscible liquids in a closed rectangular container has been studied experimentally in a physical model. Fig. 16 of [11] shows the gravity-driven interface motion between two liquids in a closed container. However, such measurements are difficult to reproduce accurately [12]. This type of free surface wave was successfully modelled by using the OpenFoam code [13]. Flows around obstacles like those added to the cathode surface have also been modelled successfully by using the OpenFoam code [14].

A similarity between the problems described above was successfully reproduced by OpenFoam. The gravity driven bath-metal interface wave in a reduction cell problem

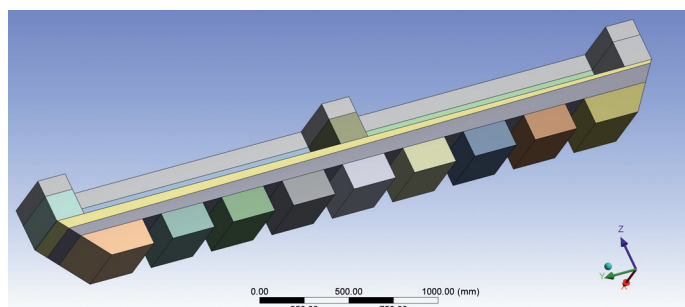


Fig. 2: Model geometries with eight continuous longitudinal ridges 160 mm high and 125 mm wide

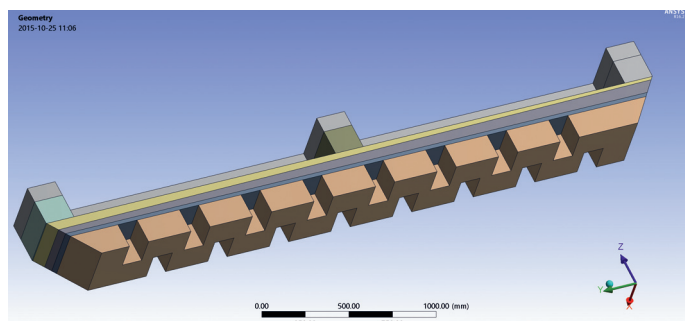


Fig. 3: Model geometries with 16 discontinuous and alternated longitudinal ridges 160 mm high and 125 mm wide

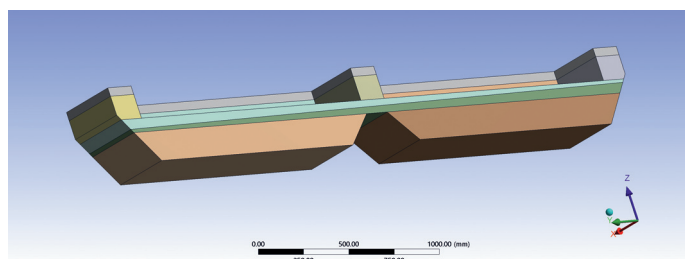


Fig. 4: Model geometries with a single trapezoidal continuous longitudinal ridge located under the centre channel

suggests that the use of OpenFoam code is appropriate for solving the proposed lateral slice model.

Setup and solution of the lateral slice model

The lateral slice model geometry is based on the cross-section of the GY420 cell design [15]. Different views of the cell design are shown in Fig. 1, which was produced from the Peter Entner CellVolt application [16]. A fairly standard bath composition was selected for this study (see Fig. 4 of [17]).

The model depth (300 mm) extended from the front frictionless symmetry plane (located at half the anode width) to the back frictionless symmetry plane (located at half the anode width between two adjacent anodes). The length (3,940 mm) of the slice model was typical of a cell cavity width of a GY420 cell, minus a 100 mm uniform ledge thickness at both sides. The height of the slice model was

a single trapezoidal continuous longitudinal ridge located under the centre channel, so leaving only 4 cm of metal pad thickness under that channel. In all the cases studies, the metal pad volume remained unchanged.

The different lateral slice model versions were modelled using a mesh of about 1,175,000 hexagonal finite volumes of fairly uniform size with an orthogonal quality of around 0.77 (see Figs 3 and 11 of [17]). The mesh density was somewhat coarser than the one used in a wind engineering study [14]. However, it was fine enough to resolve fairly well the boundary layer at the solid surfaces (cathode, anode and ledge). The mesh

was perfectly aligned with the initial position of the bath-metal interface in order to ensure a smooth start of the transient solution.

The transient solution was started with a sloped bath-metal interface of -20 mm on the left side and +20 mm on the right side of the lateral slice model. The motion of the fluids was calculated using an explicit solver available in the OpenFoam 2.3.0 code [18]. The multiphase Euler solver was used with a maximum Courant Number of 0.05 and maximum time step of 0.02 seconds. Because of its demonstrated ability to predict viscous drag fairly well, the $k-\omega$ SST (shear stress transport) turbulence model was used in the flow calculation [19]. Continuity of the velocity was assumed at the bath-metal interface.

The transient calculations were made for a total of 60 seconds, which allowed about three oscillations of the bath-metal interface. The calculations were performed on a Dell Xeon ES-2697 V3 computer having 128 GB of RAM and 28 cores. The computer took about 30 CPU hours to calculate that transient solution using all 28 cores.

composed of three layers: 200 mm for the metal pad (for the flat cathode surface case), 200 mm for the bath layer, and 75 mm as an air layer on top. The average anode-cathode distance (ACD) was 40 mm. The cathode surface was either flat or with different types of irregularities. Fig. 1 of [17] shows the geometry of the flat cathode surface case, while Fig. 10 of [17] shows the geometry of the first type of cathode surface irregularity studied, consisting of eight continuous longitudinal ridges, each 100 mm high and 200 mm wide. Figs 2-4 show the geometry of the next three new types of cathode surface irregularities studied, namely eight continuous longitudinal ridges 160 mm high and 125 mm wide, 16 discontinuous and alternating longitudinal ridges 160 mm high and 125 mm wide, representing

namely eight continuous longitudinal ridges 160 mm high and 125 mm wide, 16 discontinuous and alternating longitudinal ridges 160 mm high and 125 mm wide, representing

namely eight continuous longitudinal ridges 160 mm high and 125 mm wide, 16 discontinuous and alternating longitudinal ridges 160 mm high and 125 mm wide, representing

Solution of the 'reference' flat cathode surface model

The solution of the 'reference' flat cathode surface model is presented in Figs 6-9 of [17]. The positions of the bath-metal interface are shown at intervals of 15 seconds in Fig. 6 of [17]. Fig. 7 of [17] shows the velocity field at the front symmetry plane, which passed through the anode centre, after 15 seconds. The maximum bath velocity was about 30 mm/s. The bath flow entrained the top layer of the metal, and flow reversal occurred in the metal pad. There was a horizontal plane of zero metal velocity about 40 mm below the bath-metal interface. After 60 seconds the velocities in the bath and metal layers were less than 5 mm/s and the motion of the bath-metal

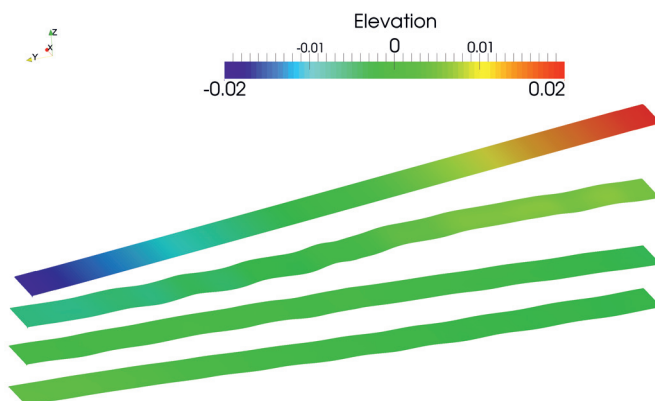


Fig. 5: Position of the bath-metal interface every 10 seconds from 0 on top to 30 seconds on bottom for the model with eight continuous rectangular 160 x 125 mm ridges

interface was almost completely damped (see Fig. 8 of [17]).

The maximum turbulent viscosity (Fig. 9 of [17]) in the metal pad was $4.66 \times 10^{-4} \text{ m}^2/\text{s}$ at 15 seconds, and was located below the centre channel. This turbulent viscosity was 1447 times higher than the laminar viscosity of molten metal at $3.22 \times 10^{-7} \text{ m}^2/\text{s}$.

Solution of the eight continuous rectangular 100 x 200 mm ridges model

Apart from the shape of the cathode surface, most of the model dimensions were kept the same as those of the ‘reference’ flat cathode surface model. However, the metal pad was raised by 41.5 mm, in order to maintain the same mass of metal, considering the extra volume of the eight continuous rectangular 100 x 200 mm ridges.

Figs 13-15 of [17] show the solution of this first irregular cathode surface model Fig. 15 of [17] shows the position of the bath-metal interface every 15 seconds. Fig. 13 of [17] shows the velocity field in the same front symmetry plane as Fig. 7 of [17] also after 15 seconds. Due to the presence of the cathode ridges, which acted like flow obstacles, the bath flow and especially the metal flow were now quite different. The bath velocity was reduced in most bath regions, and the metal pad had local regions of high and low velocities near the

cathode ridges. The horizontal plane of zero metal velocity was raised towards the bath-metal interface by about 40 mm. This modified flow field could translate into higher current efficiency.

The maximum turbulent viscosity (Fig. 14 of [17]) was reduced to $3.85 \times 10^{-4} \text{ m}^2/\text{s}$ and occupied a much smaller area beneath the centre channel. These results seem to suggest some stabilization of the bath-metal interface.

Solution for the eight continuous rectangular 160 x 125 mm ridges model

Since [17] was written, three new cathode models have been designed and solved to test different types of cathode surface irregularities (see Figs 2-4). Fig. 5 shows the position of the bath-metal interface at intervals of 10 seconds from 0 to 30 seconds for the design with eight continuous rectangular 160 x 125 mm ridges. The bath-metal interface does not move significantly after that.

Fig. 6 presents the velocity field in the front symmetry plane after 10 seconds for that same model. Due to the presence of the much higher ridges, the maximum velocity is now located in the metal pad, and the horizontal plane of flow reversal has essentially moved to the bath-metal interface. For that reason, this is possibly an improvement over the previous model solution with eight continuous rectangular 100 x 200 mm ridges.

Solution for the 16 discontinuous alternating rectangular 160 x 125 mm ridges model

The next model serves to test whether using discontinuous alternating ridges would constitute an improvement over continuous ridges. Fig. 7 shows the position of the bath-metal interface for that model after 10 seconds, starting from the same point as all the previous cases. Fig. 8 shows the metal pad velocity field after 10 seconds in a horizontal plane located 80 mm above bottom of the metal pad, which is at the mid height of the ridges. The metal flow zigzags around the discontinuous alternating ridges, which might reduce sludge formation. Fig. 9 presents the velocity field in the front symmetry plane after 10 seconds for that same model. The maximum velocity is located in the bath, and the flow reversal has now moved back down into the metal pad.

Solution for the single trapezoidal continuous ridge model

The last model aims to test the metal pad flow using a quite different type of cathode surface obstacle inspired from the recent Alcoa patent [20]. It is a single, continuous longitudinal obstacle located under the centre channel. It has a trapezoidal shape of which the top section is almost as wide as the centre channel itself and it leaves only 4 cm of metal pad thickness above it (see Fig. 4).

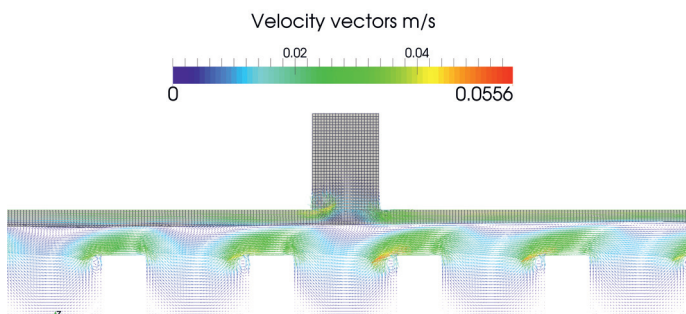


Fig. 6: Velocity field in the front symmetry plane after 10 seconds for the model with eight continuous rectangular 160 x 125 mm ridges

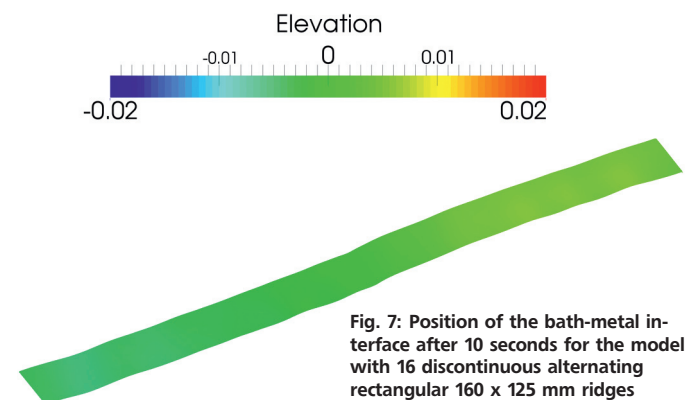


Fig. 7: Position of the bath-metal interface after 10 seconds for the model with 16 discontinuous alternating rectangular 160 x 125 mm ridges

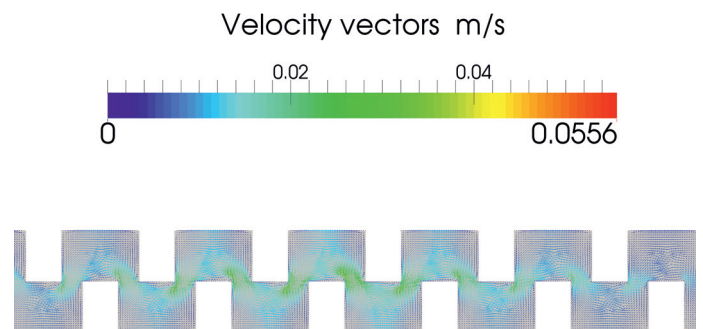


Fig. 8: Velocity field at the ridges mid height horizontal plane after 10 seconds for the model with 16 discontinuous alternating rectangular 160 x 125 mm ridges

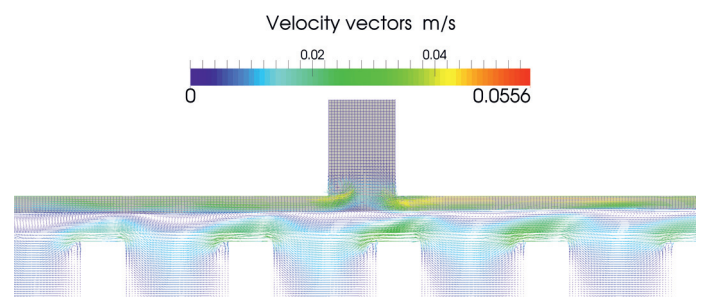


Fig. 9: Velocity field in the front symmetry plane after 10 seconds for the model with 16 discontinuous alternating rectangular 160 x 125 mm ridges

Fig. 10 shows the position of the bath-metal interface for that model after 10 seconds, starting from the same point as all the previous cases. Fig. 11 presents the velocity field in the front symmetry plane after 10 seconds for that same model. The maximum velocity is in the meal pad above the trapezoidal ridge.

Comparison of the damping rate

There was very little difference between the evolution of the interface positions for all the five cases modelled. Only the height of the small ripples on the interface varies from case to case. The amplitude of those small ripples increases when the tops of continuous ridges get closer to the interface position.

More revealing was the dynamic bath-metal interface position at the front left corner for all five models presented in Fig. 12. This clearly showed two families of curves. The evolution of corner position of the single trapezoidal continuous ridge case, as for the case of 16 discontinuous alternating ridges, is very close to the evolution of the 'reference' flat cathode surface case. For the two remaining cases, namely the eight continuous rectangular ridges, there was less overshoot for the two oscillations at 26 and 45 seconds. Also, secondary ripples of the bath-metal interface were smaller for that second group. Yet, of all five cases, the same interface positions were obtained at the same time after 50 seconds.

Clearly the presence of eight continuous rectangular ridges had some effect on the dynamic evolution of the bath-metal interface. It can also be argued that the 160 x 125 mm ridge size is very slightly more effective than the 100 x 200 mm ridge size, yet those higher and narrower ridges might erode faster.

Future work

The 3D transient lateral slice model has demonstrated that continuous longitudinal ridges stabilized the bath-metal interface somewhat. Thus additional studies seem to be warranted in order to:

- optimize the mesh size, time step, Courant Number, turbulence model, etc.
- explore other dimensions of the rectangular ridge
- explore other ridge shapes like triangular or semi-circular
- develop a 3D transient model of the entire reduction cell.

The GY420 cell design has 48 anodes. Thus a 3D transient model of that entire cell would be about 50 times bigger than the present 3D transient lateral slice model. The bath and metal layers would be subjected to time-varying MHD Lorentz forces, in addition to the constant gravity forces. Constant gas release drag forces could also be added to the bath layer.

We have already demonstrated that the OpenFoam code can handle MHD flows successfully [21, 22]. We expect that a 3D transient OpenFoam VOF formulation based cell model would be an excellent tool for the analysis of cell stability, especially to study the impact of irregular cathode surfaces.

The computing time on the same Dell Xeon ES-2697 V3 computer would be about 1500 CPU hours, or about two months. Clearly using an even faster computer with more than 28 cores would be required in order to reduce the turn around time. Even nowadays, CPU resources are still too expensive to be able to carry out such 3D transient cell stability analysis without a very significant R&D budget.

Conclusions

Lateral gravity waves were successfully simulated in a 3D transient slice model of a reduction cell. The simulation investigated the effect of the cathode surface on the bath-metal interface. The results showed that multiple continuous longitudinal ridges promote some level of extra wave damping, while other types of irregular cathode surface irregularities have no observable impact.

The lateral slice model was solved using the VOF formulation in the OpenFoam code on a Dell 28 cores Xeon ES-2697 V3 computer having 128 GB of RAM at its disposal. The calculation took about 30 CPU hours to calculate the transient evolution of the bath-metal interface during 60 seconds.

References

- [1] N. X. Feng: Low Energy Consumption Aluminum Reduction Cell with Novel Cathode, China, ZL 200710010523.4, 2008.
- [2] Q. Wang, B. Li, Z. He and N. Feng, Simulation of Magnetohydrodynamic Multiphase Flow Phenomena and Interface Fluctuation in Aluminum Electrolytic Cell with Innovative Cathode, Metallurgical and Materials Transactions B, Vol. 45B 2014, 272-294.
- [3] M. Dupuis and V. Bojarevics, Non-linear Stability Analysis of Cells Having Different Types of Cathode Surface Geometry, TMS Light Metals 2015, 821-826.

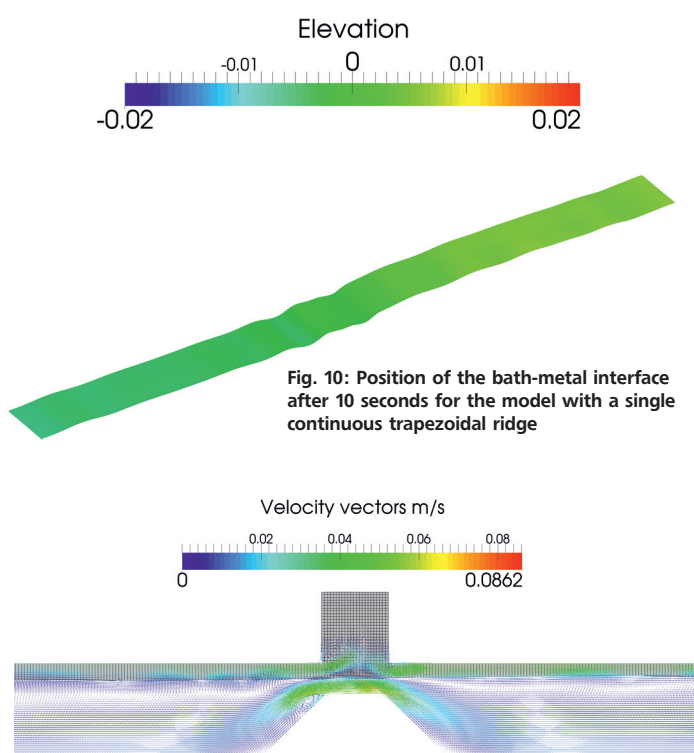


Fig. 10: Position of the bath-metal interface after 10 seconds for the model with a single continuous trapezoidal ridge

Fig. 11: Velocity field in the front symmetry plane after 10 seconds for the model with a single continuous trapezoidal ridge

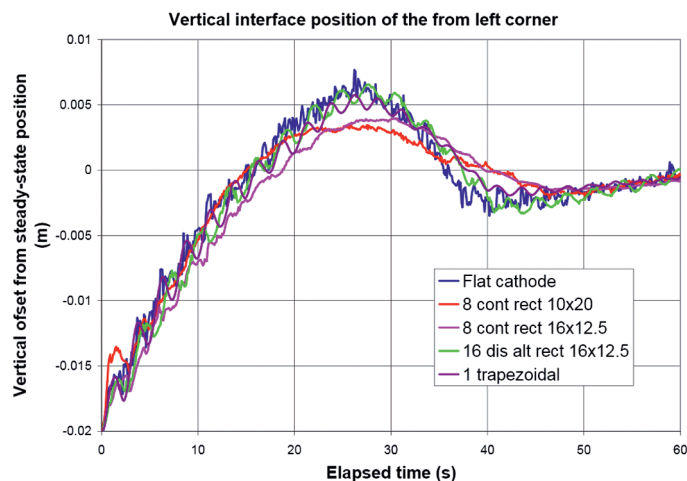


Fig. 12: The dynamic bath-metal interface position at the front left corner for all five models

- [4] M. Dupuis and V. Bojarevics, Influence of the Cathode Surface Geometry on the Metal Pad Current Density, TMS Light Metals 2014, 479-484.
- [5] M. Dupuis and V. Bojarevics, Newest MHD-Valdis Cell Stability Studies, Aluminium, 90 (2014) 1-2, 42-44.
- [6] V. Bojarevics, MHD of Aluminium Cells with the Effect of Channels and Cathode Perturbation Elements, TMS Light Metals 2013, 609-614.
- [7] N. Urata, Wave Mode Coupling and Instability in the Internal Wave in the Aluminum Reduction Cells, TMS Light Metals 2005, 455-460.
- [8] P. Davidson, An Introduction to Magnetohydrodynamics, Cambridge Texts in Applied Mathematics, Cambridge University Press 2001, 363-386.
- [9] H. Jasak, OpenFOAM: Introduction, Capabilities and HPC Needs, Cyprus Advanced HPC Workshop Winter 2012.
- [10] S. Hansch, D. Lucas, T. Hohne, E. Krepper and G. Montoya, Comparative Simulations of Free Surface Flows Using VOF-Methods and a New Approach for Multi-Scale Interfacial Structures, Proceedings of the ASME 2013 Fluids Engineering Division Summer Meeting.
- [11] S. Y. Lee¹, C. E. Park and V. H. Ransom, On The Gravity Driven Force Terms of Single Pressure One-Dimensional Multi-Fluid Flow Model in Horizontal Channel and Their Validation, Proceedings of ICAPP 2013 Jeju Island, Korea, April 14-18, 2013.
- [12] D. R. Howell, B. Buhrow, T. Heath, C. McKenna, W. Hwang and M. F. Schatza, Measurements of Surface-wave Damping in a Container, Physics of Fluids, Vol. 12, no 2, February 2000, 322-326.
- [13] G. C. J. Morgan, Application of the InterFoam VOF Code to Coastal Wave/Structure Interaction, Ph. D. thesis, University of Bath, Department of Architecture and Civil Engineering, September 2012.
- [14] I. Lindmeier, C. Heschl, G. Clauss and U. Heck, Prediction of the Flow Around 3D Obstacles Using Open Source CFD-Software, The 5th International Symposium on Computational Wind Engineering (CWE2010) Chapel Hill, North Carolina, USA May 23-27, 2010
- [15] Ji-lin DING, Jie LI, Hong-liang ZHANG, Yu-jie XU, Shuai YANG and Ye-xiang LIU, Comparison of Structure and Physical Fields in 400 kA Aluminum Reduction Cells, J. Cent. South Univ., (2014) 21, 4097-4103.
- [16] AlWeb: <http://peter-entner.com/ug/windows/cellvolt/toc.aspx>
- [17] M. Dupuis and M. Pagé, Modeling Gravity Wave in 3D with OpenFoam in an Aluminum Reduction Cell with Regular and Irregular Cathode Surfaces, TMS Light Metals 2016, to be published.
- [18] OpenFoam 2.3.0: www.openfoam.org/version2.3.0/
- [19] F. R. Menter, Review of the Shear-stress Transport Turbulence Model Experience from an Industrial Perspective, International Journal of Computational Fluid Dynamics, Vol. 23, No. 4, April-May 2009, 305-316.
- [20] Y. Ruan and al., Apparatus and Method for Improving Magneto-Hydrodynamics Stability and Reducing Energy Consumption for Aluminum Reduction Cells, US patent 2013/0032486 A1, 2013.
- [21] A. Panchal, Study of Liquid Metal MHD Flows Using OpenFOAM, AE 494:BTP Stage 2, Dept. of Aerospace Engineering, IIT Bombay.
- [22] E. Mas de les Valls, Development of a Simulation Tool for MHD Flows under Nuclear Fusion Conditions, Ph. D. thesis, Dept. of Physics and Nuclear Engineering Universitat Politècnica de Catalunya, October 2011.

Authors

Dr. Marc Dupuis is a consultant specialized in the applications of mathematical modelling for the aluminium industry since 1994, the year when he founded his own consulting company GeniSim Inc (www.genisim.com). Before that, he graduated with a Ph.D. in chemical engineering from Laval University in Quebec City in 1984, and then worked ten years as a research engineer for Alcan International. His main research interests are the development of mathematical models of the Hall-Héroult cell dealing with the thermo-electric, thermo-mechanic, electro-magnetic and hydrodynamic aspects of the problem. He was also involved in the design of experimental high amperage cells and the retrofit of many existing cell technologies.

Michaël Pagé is specialized in mechanical engineering in the field of numerical simulation. Graduated from the University of Quebec at Chicoutimi in 2006, he has since worked in digital simulation for engineering as well as product development firms. His professional experience and his personal interest in simulation have enabled him to acquire a remarkable mastery of this technology. His technical versatility allowed him to participate in several projects in the hydroelectric field in Quebec and abroad. Since 2013, he is one of the leaders of Simu-K inc., a company that offers services in digital simulation. This new challenge allows him to work with companies that are experts in their field to produce innovative solutions for their customers.